JETIR.ORG ISSN: 2349-5162 | ESTD Year : 2014 | Monthly Issue
JOURNAL OF EMERGING TECHNOLOGIES AND INNOVATIVE RESEARCH (JETIR)
An International Scholarly Open Access, Peer-reviewed, Refereed Journal

Modelling and Analysis of a Tapped-Inductor Boost Converter

Smitha Joseph
Lecturer in Electrical &Electronics Engineering,
Government Polytechnic College, Kalamassery, Kerala, India.

Abstract : This paper presents the systematic derivation, circuit modelling, and performance analysis of a tapped-inductor boost DC–DC converter obtained from the classical boost converter by replacing the input inductor with a tapped magnetic structure. The tapped inductor provides transformer-like action that increases the voltage gain without requiring extreme duty ratios, while retaining the non-isolated single-switch architecture. The linearized small-signal models derived from averaged state-space equations are the standard tool for predicting control-to-output transfer functions, and for designing compensators that guarantee stability and dynamic performance.

Index Terms **- State space modelling, Tapped inductor, magnetizing inductance, continuous conduction mode**

I. INTRODUCTION

DC–DC boost converters are essential components in power conversion systems, including photovoltaic modules, fuel cells, electric vehicles, battery-powered devices, and high-power LED drivers [1]. The classical boost converter is widely recognized due to its simple structure, and high-frequency switching capability. However, it exhibits considerable limitations when there is a demand for very high voltage gain, especially during operation at duty cycles nearing unity. Under these conditions, conduction losses increase significantly, efficiency drops sharply, and the switch voltage stress increases to impractical levels.

To overcome these constraints while maintaining a single active switch, the tapped-inductor boost converter topology was introduced [2]. In this configuration, the single input inductor of the conventional boost is replaced with a multi-turn coupled winding. The secondary winding is tapped, which offers a gain enhancement based on the turns ratio. The resulting topology can be viewed as a hybrid between a transformer-based and inductor-based design, combining high step-up capability with simple non-isolated structure.

The tapped inductor incorporates magnetizing inductance, leakage inductance, and a coupling coefficient, all of which significantly affect efficiency and dynamic performance. A lot of prior work on tapped-inductor converters has been carried out under the assumption of ideal magnetic coupling or by explicitly including leakage inductance, often resulting in higher-order and more complex models [3], [4]. In contrast, the present paper aims to model the tapped-inductor boost converter in a manner closely analogous to the conventional boost converter. This approach yields a second-order representation that is easier to use for analysis and control design.

Paper is organized as follows. Section II describes methodology to derive the steady state gain and the state space modelling similar to boost converter. After deriving the small-signal models of both the conventional boost and the tapped-inductor boost converters in Section II, the corresponding results are presented and discussed in Section III. Finally, Section IV presents conclusions.

II. METHODOLOGY

In the methodology, the linearized small-signal modelling process begins with an analysis of the conventional boost converter shown in Fig. 1, along with its ON and OFF switching states presented in Fig. 2. This basic idea is then extended to develop the small-signal model of the tapped coupled-inductor converter.

a) Linearized Small-Signal Model of Boost Converter

This section presents the derivation of the control-to-output transfer function of conventional boost converter.

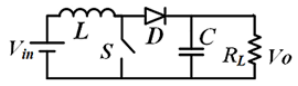

Fig. 1 Conventional Boost converter

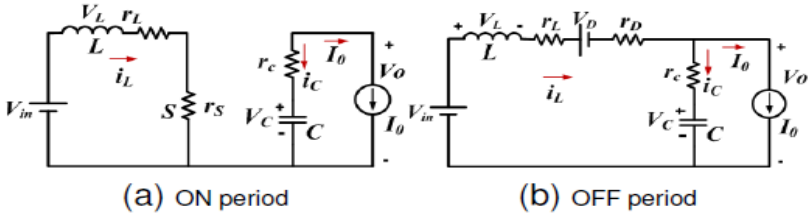

Fig. 2 ON and OFF circuit structures of conventional Boost converter

Let r_L is the resistance of inductor, r_S is the switch resistance, r_C is the ESR of capacitor, r_D is the forward resistance of the diode and V_D is the cut-in voltage of the diode.

The equations for the ON-state are presented as follows:

$$V_{LON} = V_{in} - i_L(r_L + r_S) \tag{1}$$

$$i_{CON} = -I_0, \quad V_0 = V_C - I_0 r_C \tag{2}$$

The equations for the OFF-state are presented as follows:

$$V_{LOFF} = V_{in} - V_D - V_C - i_L(r_L + r_D + r_C) + I_0 r_C \tag{3}$$

$$i_{COFF} = i_L - I_0 \tag{4}$$

$$V_0 = V_C + i_L r_C - I_0 r_C \tag{5}$$

By applying the volt-second balance principle to the above equations, the ideal voltage gain of the conventional boost converter can be derived as follows.

$$V_0/V_{in} = 1/(1-d) \tag{6}$$

The inductor current (i_L), and the output capacitor voltage (V_C) are identified as the independent state variables within the boost converter. The state-space averaged model of a boost converter in continuous conduction mode (CCM) is given below, with d_0 denoting the operating-point duty ratio.

$$\begin{bmatrix} \frac{d\overline{i_L}}{dt} \\ \frac{d\overline{v_C}}{dt} \end{bmatrix} = \begin{bmatrix} -\left(\frac{d_0 r_{on}}{L} + \frac{(1-d_0)r_{off}}{L}\right) & -\frac{(1-d_0)}{L} \\ \frac{(1-d_0)}{C} & 0 \end{bmatrix} \begin{bmatrix} \overline{i_L} \\ \overline{v_C} \end{bmatrix} + \begin{bmatrix} \frac{d_0}{L} + \frac{1-d_0}{L} & -\frac{(1-d_0)}{L} & \frac{(1-d_0)r_C}{L} \\ 0 & 0 & -\frac{1}{C} \end{bmatrix} \begin{bmatrix} \overline{v_{in}} \\ V_D \\ \overline{i_o} \end{bmatrix} \tag{7}$$

where $r_{on} = r_L + r_s$, $r_{off} = r_L + r_D + r_C$

$$\bar{v}_o = \begin{bmatrix} (1-d_0)r_C & 1 \end{bmatrix} \begin{bmatrix} \overline{i_L} \\ \overline{v_C} \end{bmatrix} + \begin{bmatrix} 0 & 0 & -r_C \end{bmatrix} \begin{bmatrix} \overline{v_{in}} \\ V_D \\ \overline{i_o} \end{bmatrix} \tag{8}$$

The non-linear model can be linearized around an operating point resulting in a linear time-invariant (LTI) model suitable for small-signal analysis. The linearized model for the boost converter is given in (9) and (10).

$$\begin{bmatrix} \dot{\Delta\overline{i_L}} \\ \dot{\Delta\overline{v_C}} \end{bmatrix} = \begin{bmatrix} -\left(\frac{d_0 r_{on}}{L} + \frac{(1-d_0)r_{off}}{L}\right) & \frac{1-d_0}{L} \\ \frac{1-d_0}{C} & 0 \end{bmatrix} \begin{bmatrix} \Delta\overline{i_L} \\ \Delta\overline{v_C} \end{bmatrix} + \begin{bmatrix} \frac{d_0}{L} + \frac{1-d_0}{L} & \frac{-(1-d_0)}{L} & \frac{(1-d_0)r_C}{L} \\ 0 & 0 & \frac{-1}{C} \end{bmatrix} \begin{bmatrix} \Delta\overline{v_{in}} \\ 0 \\ \Delta\overline{i_0} \end{bmatrix} + \begin{bmatrix} \alpha \\ \beta \end{bmatrix} [\Delta d(t)] \tag{9}$$

$$[\Delta\overline{V}_0] = \begin{bmatrix} (1-d_0)r_C & 1 \end{bmatrix} \begin{bmatrix} \Delta\overline{i}_L \\ \Delta\overline{v}_C \end{bmatrix} + \begin{bmatrix} 0 & 0 & -r_C \end{bmatrix} \begin{bmatrix} \Delta\overline{v}_{in} \\ 0 \\ \Delta\overline{i}_0 \end{bmatrix} + [\gamma] \, [\Delta\overline{d(t)}] \tag{10}$$

where $\gamma = -\frac{r_C \bar{I}_0}{(1-d_0)}$

The transfer functions from the state variables to the duty ratio is derived by setting all other inputs to zero as shown in (11) and (12).

$$\frac{\Delta\overline{i_L}(s)}{\Delta d(s)} = \frac{\alpha s - \frac{\beta(1-d_0)}{L}}{s^2 + \frac{r_{\text{eff}}}{L}s + \frac{(1-d_0)^2}{LC}} \tag{11}$$

$$\frac{\Delta\overline{v_C}(s)}{\Delta d(s)} = \frac{\beta s + \frac{\beta r_{eff}}{L} + \frac{\alpha(1-d_0)}{C}}{s^2 + \frac{r_{\text{eff}}}{L}s + \frac{(1-d_0)^2}{LC}} \tag{12}$$

where $\frac{r_{\text{eff}}}{L} = \frac{(d_0 r_{on}) + ((1-d_0)r_{off})}{L}$

In the case of a boost converter, the output voltage V_0 is higher. In comparison to V_0, parasitic resistance voltage drops can be neglected. Therefore, the terms α, β, and γ can be approximated as follows.

$$\alpha \approx \frac{V_0}{L} \ , \ \beta = \frac{-I_0}{C(1-d_0)} \ , \ \gamma \approx 0 \tag{13}$$

In a similar way of equations (11) and (12), the control-to-output transfer function can be derived and is shown in (14).

$$\frac{\Delta\overline{V}_0(s)}{\Delta d(s)} = \frac{\beta s + \frac{\beta r_{eff}}{L} + \frac{\alpha(1-d_0)}{C}}{s^2 + \frac{r_{\text{eff}}}{L}s + \frac{(1-d_0)^2}{LC}} \tag{14}$$

The final control-to-output transfer function of boost converter is given in (15).

$$\frac{\Delta\overline{V_0}(s)}{\Delta d(s)} = \frac{\frac{(1-d_0)}{C}\frac{V_0}{L} - \frac{I_0}{C(1-d_0)}s}{s^2 + \frac{r_{\text{eff}}}{L}s + \frac{(1-d_0)^2}{LC}} = \left(\frac{(1-d_0)V_0}{LC}\right) \frac{\left(1 - s\frac{LI_0}{(1-d_0)^2 V_0}\right)}{\left(s^2 + \frac{r_{\text{eff}}}{L}s + \frac{(1-d_0)^2}{LC}\right)} \tag{15}$$

b) Linearized Small-Signal Model of Tapped Inductor Boost Converter

The inductor in the boost converter can now be replaced with a coupled inductor to enhance the voltage gain by taking advantage of its turns ratio. The primary and secondary windings of the tapped inductor is connected in series, as shown in Fig. 3.

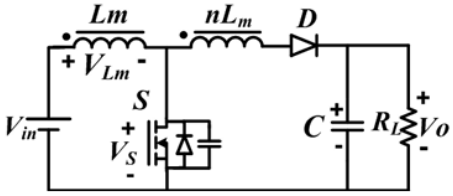

Fig. 3 Series connected tapped inductor boost converter

Consider the ON and OFF circuit configurations of the series-connected tapped inductor boost converter, including parasitic elements, as depicted in Fig. 4.

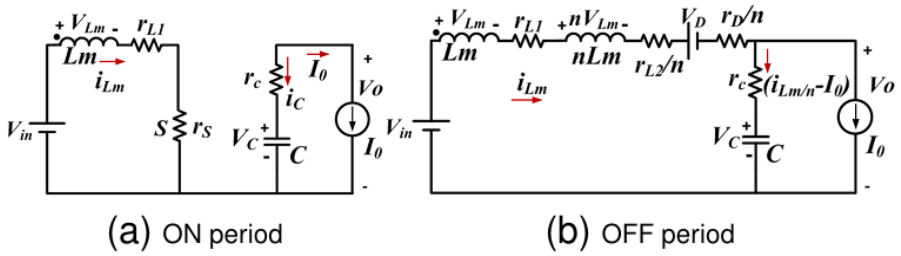

Fig. 4 ON and OFF periods of series connected tapped inductor boost converter

The primary inductance of the tapped inductor is denoted as *Lm*, while the secondary inductance is expressed as *nLm*, where *n* is the turns ratio of the tapped inductor. The independent state variables are the magnetizing inductance current, i_{Lm} and the voltage across the output capacitor, V_C. The state-space averaged model is derived by applying Kirchhoff's voltage and current laws to the ON and OFF circuit configurations. The ON-state equations are given below:

$$V_{LmON} = V_{in} - i_{Lm}\,(r_{L1} + r_S) \tag{16}$$

$$i_{CON} = -I_0 \tag{17}$$

$$V_0 = V_C - I_0 r_C \tag{18}$$

The OFF-state equations are given below:

$$(n+1)V_{LmOFF} = V_{in} - V_D - V_C + I_0 r_C - i_{Lm}\left(r_{L1} + \frac{r_{L2}}{n} + \frac{r_D}{n} + \frac{r_C}{n}\right) \tag{19}$$

$$i_{COFF} = \frac{i_{Lm}}{n} - I_0 \tag{20}$$

$$V_0 = V_C + \frac{i_{Lm} r_C}{n} - I_0 r_C \tag{21}$$

By applying the volt-second balance principle to the above equations, the ideal voltage gain of the tapped inductor boost converter can be derived as follows.

$$V_0/V_{in} = (1 + nd)/(1 - d) \tag{22}$$

The ON period is identical to that of a conventional boost converter, while during the OFF period, the elements discharge in series to achieve a high voltage gain. The state equations are derived as presented in (23) and (24).

$$\begin{bmatrix} \frac{d\overline{i_{Lm}}}{dt} \\ \frac{d\overline{v_C}}{dt} \end{bmatrix} = \begin{bmatrix} -\left(\frac{d_0 r_{on}}{L_{on}} + \frac{(1-d_0) r_{off}}{L_{off}}\right) & -\frac{(1-d_0)}{L_{off}} \\ \frac{(1-d_0)}{nC} & 0 \end{bmatrix} \begin{bmatrix} \overline{i_{Lm}} \\ \overline{v_C} \end{bmatrix} + \begin{bmatrix} \frac{d_0}{L_{on}} + \frac{1-d_0}{L_{off}} & -\frac{(1-d_0)}{L_{off}} & \frac{(1-d_0) r_C}{L_{off}} \\ 0 & 0 & -\frac{1}{C} \end{bmatrix} \begin{bmatrix} \overline{v_{in}} \\ V_D \\ \overline{i_o} \end{bmatrix} \tag{23}$$

where $L_{on} = L_m, L_{off} = (n+1)L_m, r_{on} = r_{L1} + r_s, r_{off} = r_{L1} + r_{L2}/n + r_D/n + r_C/n$

$$\bar{v}_o = \begin{bmatrix} (1-d_0)\frac{r_C}{n} & 1 \end{bmatrix} \begin{bmatrix} \overline{i_{Lm}} \\ \overline{v_C} \end{bmatrix} + \begin{bmatrix} 0 & 0 & -r_C \end{bmatrix} \begin{bmatrix} \overline{v_{in}} \\ V_D \\ \overline{i_o} \end{bmatrix} \tag{24}$$

$$\alpha \approx \frac{V_0}{L_{off}}\,,\ \gamma \approx 0 \tag{25}$$

$$\beta = \frac{-\text{Gain}.I_0}{nC} \text{ , where Gain} = \frac{1+nd_0}{1-d_0} \tag{26}$$

The control-to-output transfer function of the series-connected tapped-inductor boost converter is derived in a manner similar to that of the conventional boost converter. The resulting control-to-output transfer function is given below.

$$\frac{\Delta\overline{V_0}(s)}{\Delta d(s)} = \frac{V_o(1-d_0)}{(n+1)L_m.nC} \frac{\left(1 - s\frac{(1+nd_0)(n+1)L_m I_0}{(1-d_0)^2 V_0}\right)}{\left(s^2 + \left(\frac{d_0 r_{on}}{L_m} + \frac{(1-d_0)r_{off}}{(n+1)L_m}\right)s + \frac{(1-d_0)^2}{nC.(n+1)L_m}\right)} \tag{27}$$

Compared to a conventional boost converter, the presence of the tapped inductor with turns ratio n modifies both the dynamic behavior and gain of the system. In (27), the numerator introduces a zero, while the denominator is a second-order polynomial representing the dynamic poles of the system, which include both damping and natural frequency terms. The transfer function structure reflects a typical second-order system with a zero in the right half-plane (RHP), common in boost and boost derived converters, which can limit control bandwidth and phase margin.

III. RESULTS AND DISCUSSION

The analysis begins with a comparison of the voltage gain characteristics of the conventional boost converter and the series-connected tapped-inductor boost converter. The design parameters of the tapped-inductor boost converter are as follows: the magnetizing inductance *Lm* is chosen as 40×10^{-6} H, and the coupled inductor has a turns ratio n =1. The steady-state duty cycle is set to d_0=0.55. The output filter capacitor $C$is selected as 400×10^{-6} F to limit the output voltage ripple. The parasitic resistances of the switch, diode, and the primary and secondary inductances are each taken as $0.05\ \Omega$.

Voltage Gain Comparison of Boost and Tapped-Inductor Boost Converters

The plot in Fig. 5 compares the voltage gain of a conventional boost converter with that of a tapped-inductor boost converter. The goal is to observe how the gain varies with the duty cycle d, and how the turns ratio $n$of the tapped inductor influences the gain performance.

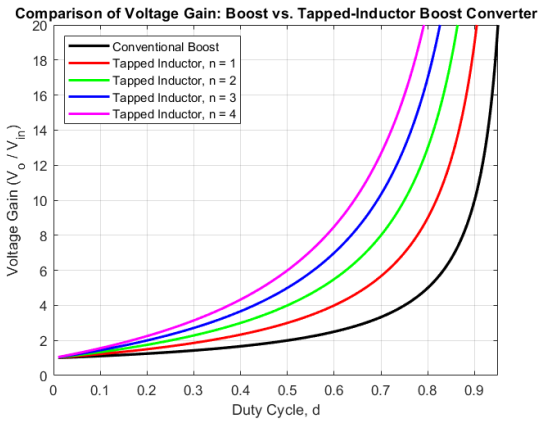

Fig. 5 Comparison of ideal voltage gain equations

Figure 6 shows the various waveforms of boost converter and Fig. 7 compares the output voltage obtained from the MATLAB/Simulink model with that from the derived transfer-function model. The two responses match closely, indicating that the mathematical model accurately represents the converter and validates the simulation results.

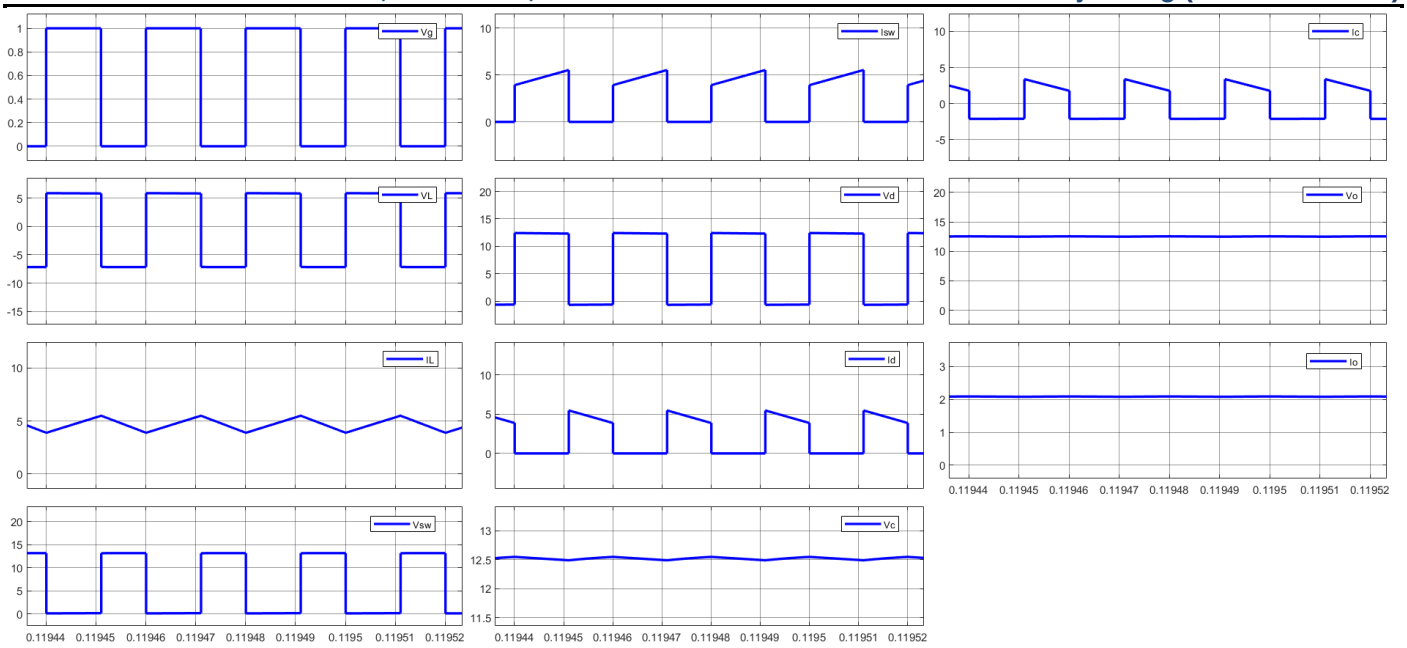

Fig. 6 Various waveforms of boost converter

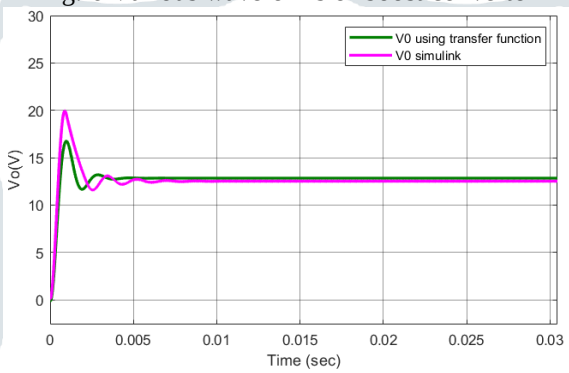

Fig. 7 Output voltage comparison: transfer-function model vs. Simulink.

Figure 8 shows the various waveforms of the tapped-inductor boost converter with a turns ratio of one. From the output voltage waveform, it can be observed that the output voltage is higher than that of the conventional boost converter due to the effect of the turns ratio. However, voltage spikes appear as a result of leakage inductance, so an appropriate energy-recovery or snubber circuit is required for tapped-inductor–based converters.

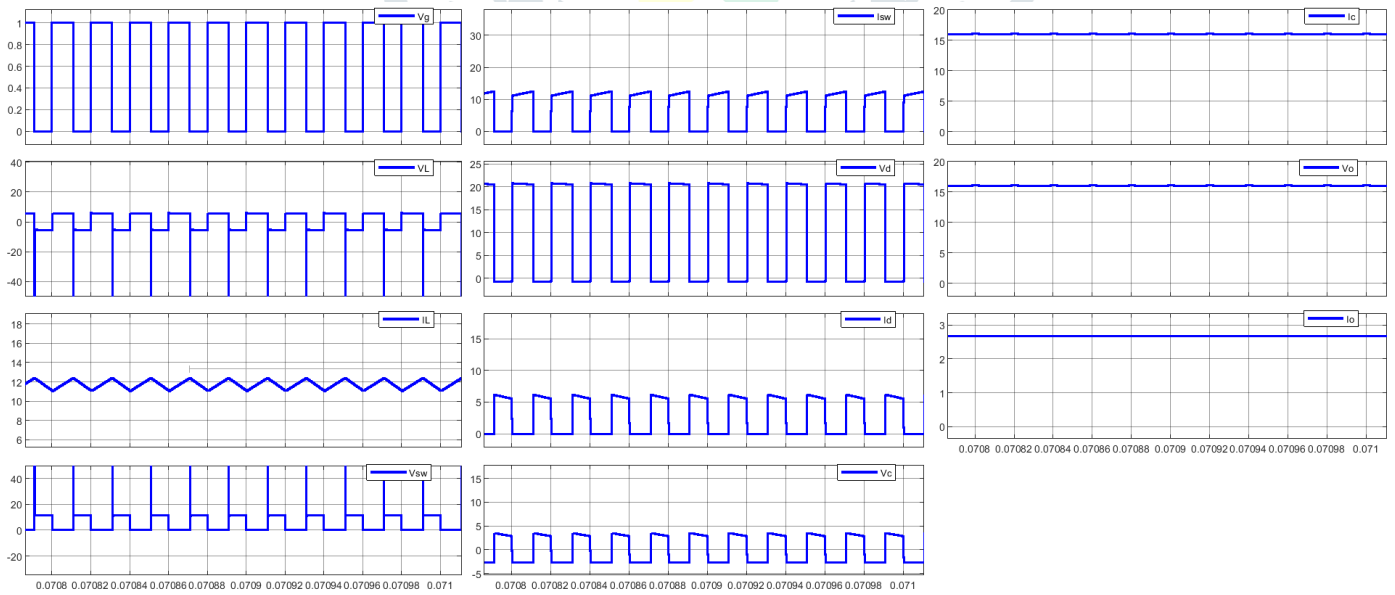

Fig. 8 Various waveforms of series connected tapped inductor boost converter

Figure 9 compares the output voltage obtained from the MATLAB/Simulink model with that from the derived transfer-function model of series connected tapped inductor. The two responses match closely, indicating that the mathematical model accurately represents the converter and validates the simulation results.

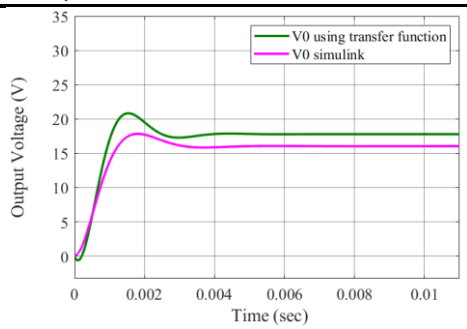

Fig. 9 Output voltage comparison: transfer-function and Simulink model of tapped inductor boost converter

IV. CONCLUSIONS

The derived second-order transfer function effectively captures the dominant dynamics of the system, including the natural frequency and damping ratio, which are essential for evaluating converter performance and stability. This model simplifies the controller design process by providing an accurate representation of the converter's response to input variations and external disturbances. Moreover, the modeling approach is scalable and can be extended to higher-order tapped-inductor configurations, enabling further analysis and optimization of advanced high-gain converter topologies.

REFERENCES

[1] F. Mumtaz, N. Z. Yahaya, S. T. Meraj, B. Singh, R. Kannan, and O. Ibrahim, "Review on non-isolated DC–DC converters and their control techniques for renewable energy applications," *Ain Shams Engineering Journal*, vol. 12, no. 4, pp. 3747–3763, 2021, doi: 10.1016/j.asej.2021.03.022.

[2] F. L. Tofoli, D. de C. Pereira, W. J. de Paula, and D. de S. Oliveira Júnior, "Survey on non-isolated high-voltage step-up DC–DC topologies based on the boost converter," IET Power Electronics, vol. 8, no. 10, pp. 2044–2057, 2015, doi: 10.1049/iet-pel.2014.0605.

[3] K. Patidar, "Tapped-inductor Quasi-z-source Based PWM DC-DC Converter," 2018 5th IEEE Uttar Pradesh Section International Conference on Electrical, Electronics and Computer Engineering (UPCON), 2018, pp. 1–6, doi: 10.1109/UPCON.2018.8597111.

[4] F. Himmelstoss and M. Windisch, "Tapped inductor Boost with exploitation of the stray energy," 2022 IEEE 20th International Power Electronics and Motion Control Conference (PEMC), Brasov, Romania, 2022, pp. 75-80, doi: 10.1109/PEMC51159.2022.9962849.